Received: 4 August 2018 | Revised: 19 October 2018 | Accepted: 19 October 2018

DOI: 10.1002/aoc.4701



FULL PAPER

WILEY Applied Organometallic Chemistry

# Synthesis and application of novel 1,2,3-triazolylferrocene-containing ionic liquid supported on $Fe_3O_4$ nanocatalyst in the synthesis of new pyran-substituted Betti bases

Mahdi Gholamhosseini-Nazari[1] | Somayeh Esmati[1] | Kazem D. Safa[1] | Alireza Khataee[2] | Reza Teimuri-Mofrad[1]

[1]Department of Organic and Biochemistry, Faculty of Chemistry, University of Tabriz, Tabriz 5166614766, Iran

[2]Research Laboratory of Advanced Water and Wastewater Treatment Processes, Department of Applied Chemistry, Faculty of Chemistry, University of Tabriz, 51666-16471 Tabriz, Iran

**Correspondence**
Kazem D. Safa, Department of Organic and Biochemistry, Faculty of Chemistry, University of Tabriz, Tabriz 5166614766, Iran.
Email: dsafa@tabrizu.ac.ir

**Funding information**
University of Tabriz

A novel magnetic ferrocene-labelled ionic liquid based on triazolium, $[Fe_3O_4@SiO_2@Triazol\text{-}Fc][HCO_3]$, has been synthesized and has been successfully introduced as a recyclable heterogeneous nanocatalyst. The catalytic activity of the novel magnetic nanoparticles was evaluated in the one-pot three-component synthesis of a wide variety of Betti bases. A simple, facile and highly efficient green method has been developed for the synthesis of kojic acid-containing Betti base derivatives at room temperature. Additionally, this new protocol has notable advantages such as short reaction times, green reaction conditions, high yields and simple workup and purification steps. Also, the novel nanocatalyst could be easily recovered using an external magnetic field and reused for six consecutive reaction cycles without significant loss of activity. The newly synthesized nanocatalyst was characterized using Fourier transform infrared spectroscopy, X-ray diffraction, energy-dispersive X-ray spectroscopy, field emission scanning electron microscopy, transmission electron microscopy and Brunauer–Emmett–Teller measurements.

**KEYWORDS**
Betti base, ferrocene, kojic acid, magnetic nanocatalyst, triazole

## 1 | INTRODUCTION

In recent years, supported heterogeneous catalysts as reusable and environmentally friendly materials have played a key role in modern science and technology, especially in organic syntheses.[1–3] Because of the advantages of catalysts immobilized on solid supports, such as easy handling, non-toxicity, low solubility and increased selectivity, these types of heterocatalysts have been widely studied.[4] Catalysts immobilized on nanostructure supports are more attractive because of their higher activity, selectivity and easy recyclability.[5–7]

Nowadays, magnetic nanoparticles are applied in various industrial and biological fields such as bioseparations, drug delivery, magnetic resonance imaging, hyperthermia and catalytic processes.[8–15]

Multicomponent reactions have major roles in organic synthesis[16] because of their advantages such as high atom efficiency, environmental friendliness, time and energy saving and quick and simple performance.[17–20] One of the important multicomponent reactions is the Betti reaction which was introduced by Mario Betti.[21,22] After the initial report of the synthesis of Betti bases, the study of these compounds has become an important area,[23–26] because of their significant biological,[27,28] synthetic[29–32] and catalytic[33] applications.

Pyran-annulated heterocyclic compounds have attracted considerable attention because of their various

  

useful biological and pharmaceutical activities. Pyrans and fused pyran derivatives are known to exhibit anti-HIV,[34] antifungal,[35] antimicrobial,[36] antiviral and anti-inflammatory,[37] antidiabetic[38] and antioxidant[39] activities. Additionally, pyran-based scaffolds show promising anticancer activities which encouraged many researchers to investigate the synthesis of these types of compounds as antitumour drug candidates.[40] Kojic acid and its derivatives are an important class of pyran-annulated heterocycles which can be found in natural and synthetic compounds.[41,42] Therefore, the development of novel methods for the efficient and convenient

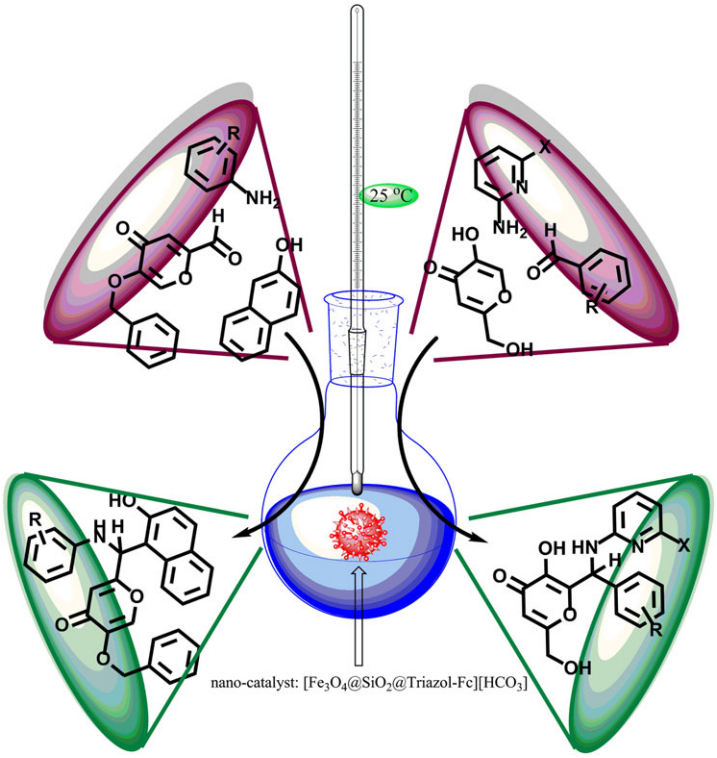


**SCHEME 1** Three-component synthesis of pyran-substituted Betti bases catalysed by $[Fe_3O_4@SiO_2@Triazol\text{-}Fc][HCO_3]$ nanocatalyst at room temperature

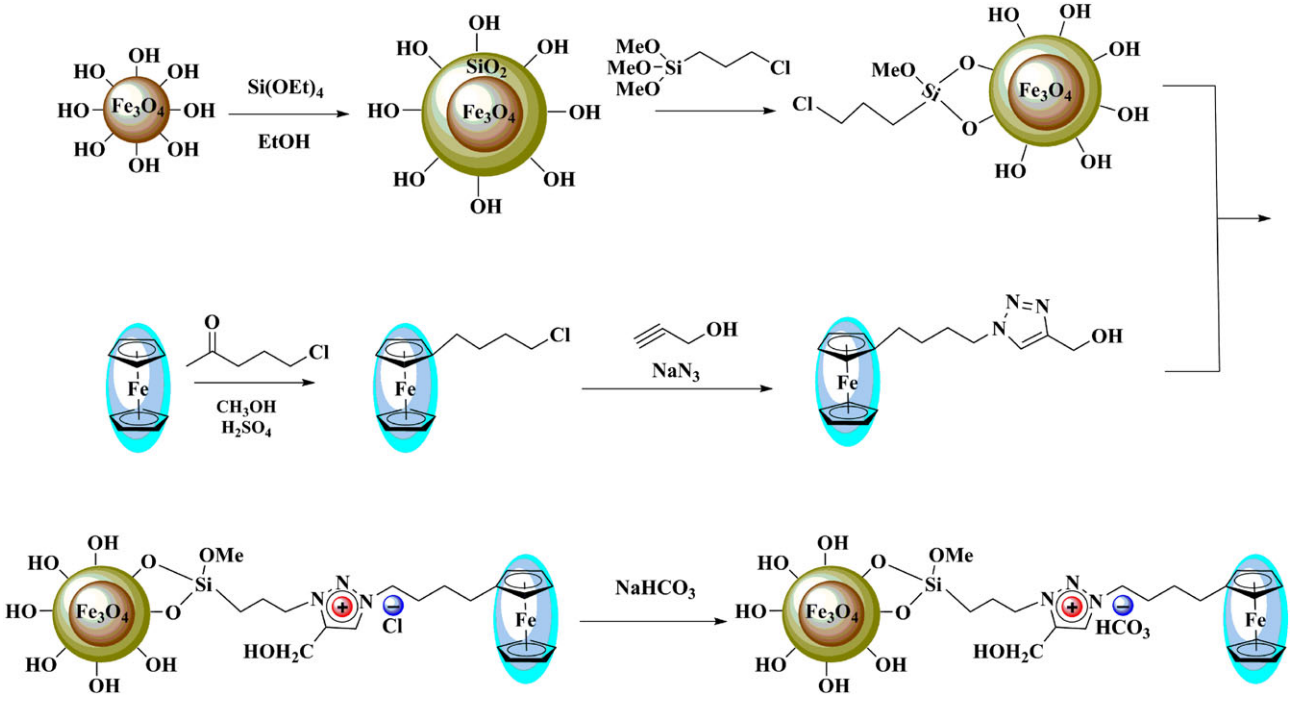


**SCHEME 2** Synthesis of $[Fe_3O_4@SiO_2@Triazol\text{-}Fc][HCO_3]$ nanoparticles

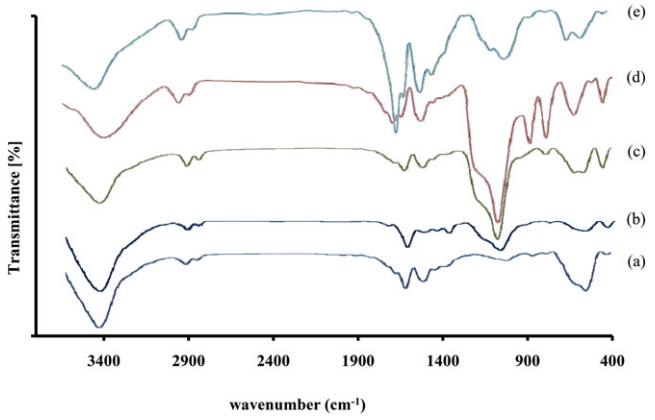


**FIGURE 1** FT-IR spectra of (a) $Fe_3O_4$, (b) $Fe_3O_4@SiO_2$, (c) $Fe_3O_4@SiO_2@(CH_2)_3Cl$, (d) $[Fe_3O_4@SiO_2@Triazol\text{-}Fc][Cl]$ and (e) $[Fe_3O_4@SiO_2@Triazol\text{-}Fc][HCO_3]$ nanoparticles

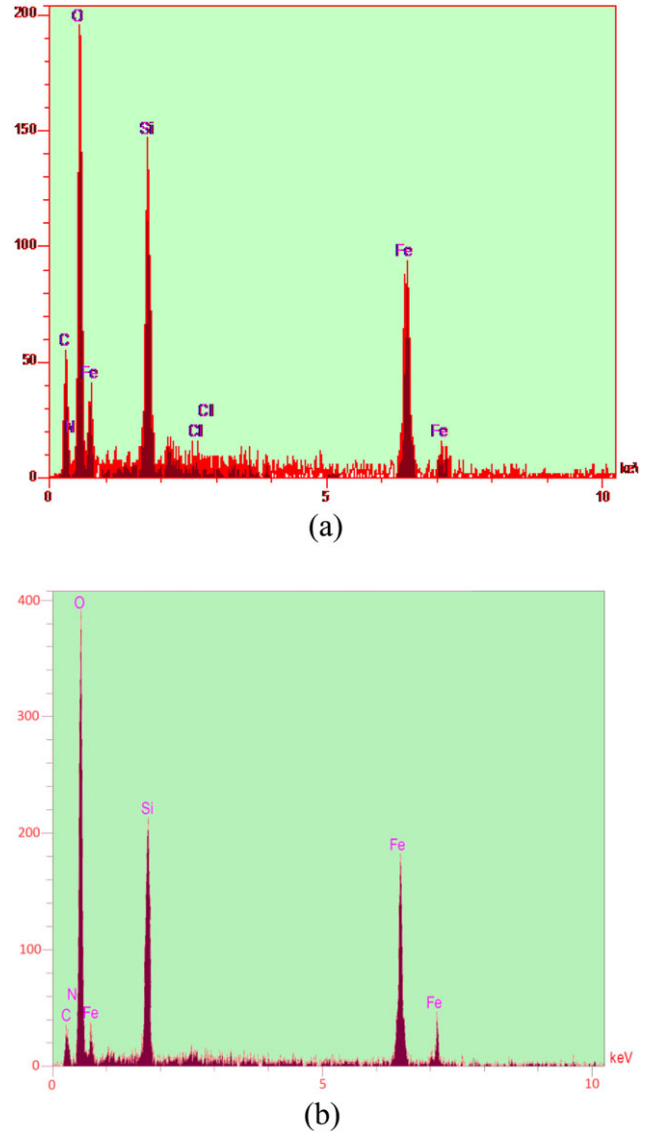


**FIGURE 2** EDX analysis of (a) $[Fe_3O_4@SiO_2@Triazol\text{-}Fc][Cl]$ and (b) $[Fe_3O_4@SiO_2@Triazol\text{-}Fc][HCO_3]$

synthesis of libraries of these compounds is an important field for modern medicinal and combinatorial chemists.

In continuation of our recent studies on the modification and development of multicomponent reactions,[43,44] and the design and synthesis of ferrocene-containing magnetic nanocatalysts[45–48] and Betti bases,[49–53] herein we introduce a new 1,2,3-triazolylferrocene-containing ionic liquid nanocatalyst stabilized on silica-coated $Fe_3O_4$ ($[Fe_3O_4@SiO_2@Triazol\text{-}Fc][HCO_3]$). We also report a simple and efficient protocol for the three-component one-pot synthesis of pyran-containing Betti base derivatives catalysed by $[Fe_3O_4@SiO_2@Triazol\text{-}Fc][HCO_3]$ at room temperature (Scheme 1).

## 2 | RESULTS AND DISCUSSION

This research was performed in two stages. The first challenge of this work was the synthesis of the $[Fe_3O_4@SiO_2@Triazol\text{-}Fc][HCO_3]$ nanocatalyst. In the second stage, pyran-containing Betti base derivatives were

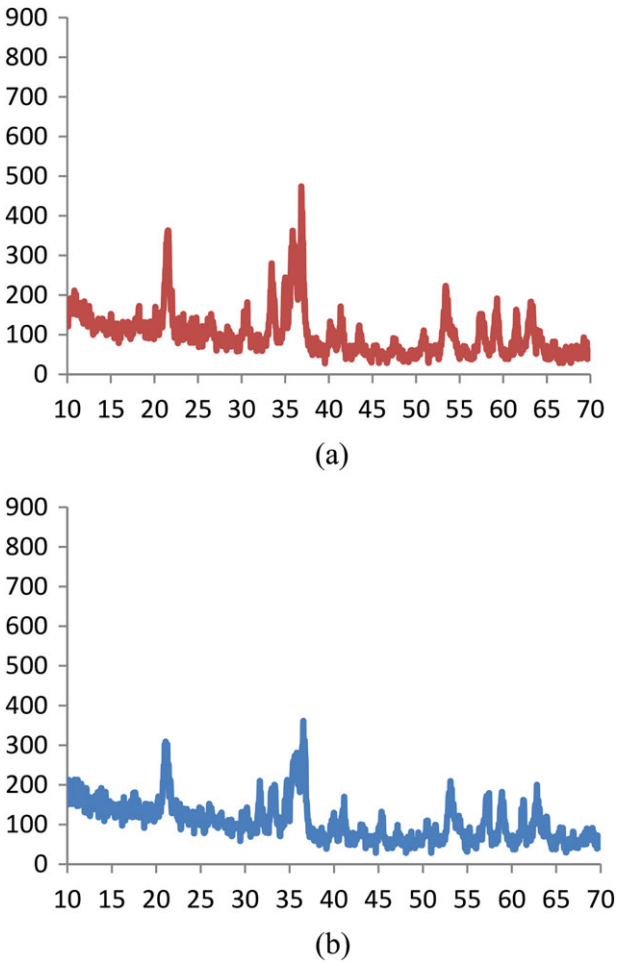


**FIGURE 3** XRD patterns of (a) $[Fe_3O_4@SiO_2@Triazol\text{-}Fc][Cl]$ and (b) $[Fe_3O_4@SiO_2@Triazol\text{-}Fc][HCO_3]$

successfully synthesized using the [$Fe_3O_4$@$SiO_2$@Triazol-Fc][$HCO_3$] nanocatalyst at room temperature.

Initially, magnetite ($Fe_3O_4$) nanoparticles were prepared and coated with $SiO_2$ and subsequently modified by (3-chloropropyl)trimethoxysilane according to reported procedures.[46,47] Then, cycloaddition reaction of 4-chlorobutylferrocene, propargyl alcohol and sodium azide afforded (1-(4-ferrocenylbutyl)-1*H*-1,2,3-triazol-4-yl) methanol. Then the reaction of $Fe_3O_4$@$SiO_2$-$(CH_2)_3Cl$ with 1,2,3-triazolylferrocene derivative produced the [$Fe_3O_4$@$SiO_2$@Triazol-Fc][$HCO_3$] nanocatalyst (Scheme 2). Chemical analysis of novel [$Fe_3O_4$@$SiO_2$@Triazol-Fc][$HCO_3$] nanoparticles was conducted using Fourier transform infrared (FT-IR) spectroscopy, X-ray diffraction (XRD), energy-dispersive X-ray (EDX) analysis, field emission scanning electron microscopy (FE-SEM), transmission electron microscopy (TEM) and Brunauer–Emmett–Teller (BET) analysis.

The FT-IR spectra of $Fe_3O_4$, $Fe_3O_4$@$SiO_2$, $Fe_3O_4$@$SiO_2$@$(CH_2)_3Cl$, [$Fe_3O_4$@$SiO_2$@Triazol-Fc][Cl] and [$Fe_3O_4$@$SiO_2$@Triazol-Fc][$HCO_3$] nanoparticles are shown in Figure 1. The absorption peaks at about 635 $cm^{-1}$ are related to Fe&bond;O bond vibrations. The absorption peaks at about 1079 $cm^{-1}$ for all $Fe_3O_4$@$SiO_2$ core–shell magnetic nanoparticles are related to the asymmetric stretching vibrations of Si&bond;O&bond;Si. In the FT-IR spectrum of [$Fe_3O_4$@$SiO_2$@Triazol-Fc][Cl] the absorption peaks at 1643 and 1549 $cm^{-1}$ are due to the stretching vibration of C&dbond;N and C&dbond;C bonds on aromatic rings. In addition, at 2923 $cm^{-1}$ the asymmetric stretching vibration of aliphatic C&bond;H appeared. An absorption peak appeared at above 3000 $cm^{-1}$ related to the stretching vibration of aromatic C&bond;H on triazol and ferrocene groups. Finally, the absorption peak at about 3400 $cm^{-1}$ is related to O&bond;H group vibrations. Accordingly, in FT-IR spectrum of the [$Fe_3O_4$@$SiO_2$@Triazol-Fc][$HCO_3$] nanoparticles, related absorption peaks appeared and, especially at about 1700 $cm^{-1}$, the absorption peak related to the vibration of the $HCO_3$ group appeared, which confirmed the successful synthesis of target nanoparticles.

EDX analyses of [$Fe_3O_4$@$SiO_2$@Triazol-Fc][Cl] and [$Fe_3O_4$@$SiO_2$@Triazol-Fc][$HCO_3$] nanoparticles are presented in Figure 2. In the EDX spectrum of the newly synthesized nanocatalyst the expected elements (C, N, O, Si and Fe) in their regions appeared and showed the true composition of the nanocatalyst. The absence of Cl

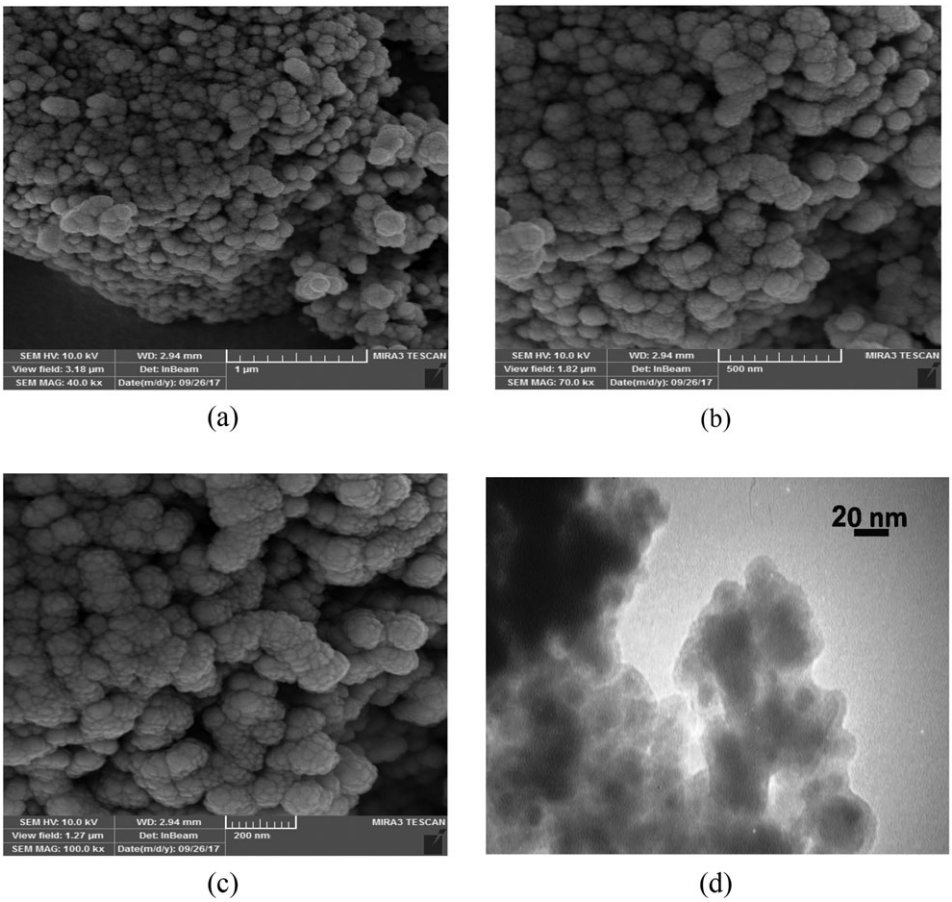


**FIGURE 4** (a–c) FE-SEM images and (d) TEM image of [$Fe_3O_4$@$SiO_2$@Triazol-Fc][$HCO_3$] nanocatalyst

in the EDX spectrum of the final nanocatalyst confirmed the successful synthesis of nanoparticles.

The XRD patterns of $[Fe_3O_4@SiO_2@Triazol\text{-}Fc][Cl]$ and $[Fe_3O_4@SiO_2@Triazol\text{-}Fc][HCO_3]$ nanoparticles were recorded at 10° to 70°. As shown in Figure 3, the XRD patterns of nanocatalysts show the crystalline dispersions of $Fe_3O_4$ magnetic nanoparticles (JCPDS card no. 85-1436). The appearance of the same peaks in the $Fe_3O_4$ and $[Fe_3O_4@SiO_2@Triazol\text{-}Fc][HCO_3]$ XRD patterns showed that the intended nanoparticles have spinel structures and, during the functionalization processes, phase change of $Fe_3O_4$ did not occur.

The peak width (full width at half maximum, FWHM), size and interplanar distance from the XRD pattern of the $[Fe_3O_4@SiO_2@Triazol\text{-}Fc][HCO_3]$ nanocatalyst were investigated. Crystallite sizes obtained from several diffraction lines using the Debye–Scherrer equation were found to be in the nanometre range, which is mainly in good agreement with the FE-SEM and TEM results. For example, measurements for the main diffraction line, 35.62°, reveal a crystalline size for the catalyst of 28.5 nm using the Debye–Scherrer equation: $D = 0.9\lambda/(\beta \cos\theta)$, where $D$ is the crystallite size, $\lambda$ is the X-ray wavelength (Cu K$\alpha$, 1.54 Å), $\beta$ is the FWHM of the diffraction peak and $\theta$ is the Bragg diffraction angle in degrees.

The surface morphology and particle size of $[Fe_3O_4@SiO_2@Triazol\text{-}Fc][HCO_3]$ nanoparticles were evaluated using FE-SEM analysis (Figure 4a–c). The FE-SEM images of the nanocatalyst showed that the shapes of nanoparticles are spherical with non-smooth surfaces which increase the surface-to-volume ratio and cause an improvement in catalytic activity of the nanoparticles. The $[Fe_3O_4@SiO_2@Triazol\text{-}Fc][HCO_3]$ nanocatalyst was also characterized using TEM and the results are shown in Figure 4d. The TEM image of the nanocatalyst confirmed that the shapes of nanoparticles are spherical. Also the core–shell structure of nanoparticles was observed in the TEM image which demonstrates the successful synthesis of the nanocatalyst. According to TEM and FE-SEM results the particles are relatively monodisperse and have a uniform size distribution around 30 nm.

We investigated the catalytic activity of the newly synthesized $[Fe_3O_4@SiO_2@Triazol\text{-}Fc][HCO_3]$ nanocatalyst

**TABLE 1** Optimization of solvent and amount of $[Fe_3O_4@SiO_2@Triazol\text{-}Fc][HCO_3]$ nanocatalyst[a]

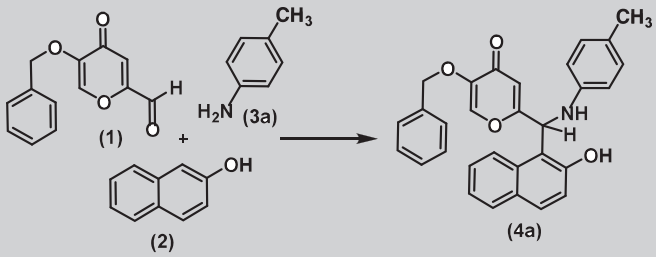


| Entry | Catalyst (amount, mg) | Solvent | Time (min) | Yield (%)[b] |
|---|---|---|---|---|
| 1 | — | — | 180 | Trace |
| 2 | [BuMeIm][Cl] (10) | — | 120 | 15 |
| 3 | [BuMeIm][$BF_4$] (10) | — | 120 | 12 |
| 4 | [BuMeIm][$PF_6$] (10) | — | 120 | 12 |
| 5 | [BuMeIm][$HCO_3$] (10) | — | 120 | 20 |
| 6 | A (10) | — | 120 | 30 |
| 7 | A (10) | $CHCl_3$ | 120 | 15 |
| 8 | A (10) | $CH_2Cl_2$ | 120 | 20 |
| 9 | A (10) | EtOH | 90 | 54 |
| 10 | A (10) | $H_2O$ | 120 | 30 |
| 11 | A (10) | EtOH–$H_2O$ (1:1) | 60 | 60 |
| 12 | A (10) | EtOH–$H_2O$ (2:1) | 50 | 85 |
| **13** | **A (10)** | **EtOH–$H_2O$ (3:1)** | **40** | **96** |
| 14 | A (5) | EtOH–$H_2O$ (3:1) | 60 | 65 |
| 15 | A (15) | EtOH–$H_2O$ (3:1) | 40 | 90 |

[a]Reaction conditions: kojic aldehyde/2-naphthol/4-methylaniline (1:1:1.1); catalyst A: $[Fe_3O_4@SiO_2@Triazol\text{-}Fc][HCO_3]$.

[b]Isolated yield.

in the synthesis of kojic acid-containing Betti bases. Initially, the reaction of kojic aldehyde (**1**), 2-naphthol (**2a**) and 4-methylaniline (**3a**) was chosen as a model reaction to optimize the reaction conditions. In this context, the efficiency of the $[Fe_3O_4@SiO_2@Triazol\text{-}Fc][HCO_3]$ nanocatalyst was investigated in various solvents, at

**TABLE 2** Synthesis of 2-hydroxynaphthalenyl(arylamino)methyl-4*H*-pyran-4-one derivatives using 10 mg of $[Fe_3O_4@SiO_2@Triazol\text{-}Fc][HCO_3]$ nanocatalyst

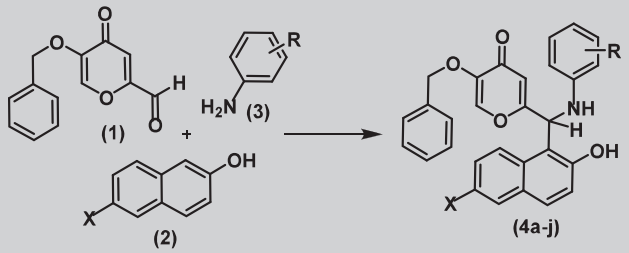


| Entry | Product | Time (min) | Yield (%) | Obs. m.p. (°C) | Lit. m.p. (°C) |
|---|---|---|---|---|---|
| 1 | 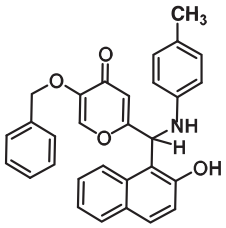 (4a) | 40 | 96 | 134–136 | — |
| 2 | 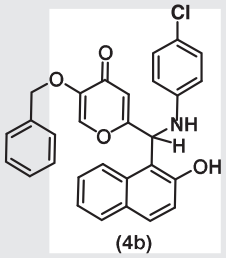 (4b) | 40 | 94 | 145–147 | — |
| 3 | 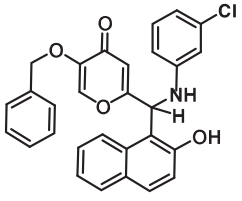 (4c) | 45 | 90 | 138–140 | — |
| 4 | 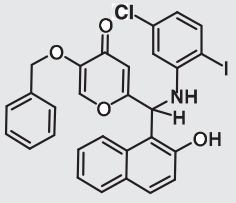 (4d) | 40 | 92 | 158–160 | — |
| 5 | 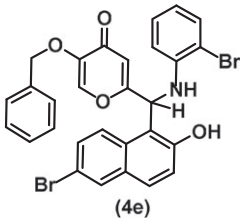 (4e) | 45 | 88 | 152–154 | — |

(Continues)

**TABLE 2** (Continued)

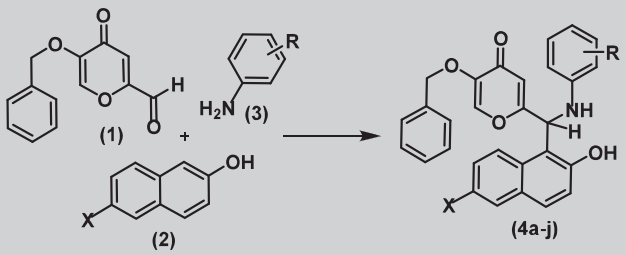


| Entry | Product | Time (min) | Yield (%) | Obs. m.p. (°C) | Lit. m.p. (°C) |
|---|---|---|---|---|---|
| 6 | 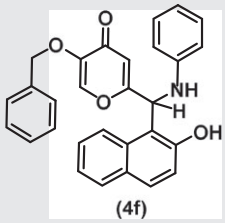 (4f) | 50 | 86 | 122–124 | 123–125[49] |
| 7 | 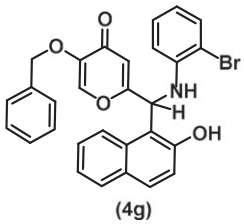 (4g) | 50 | 85 | 143–145 | 144–146[49] |
| 8 | 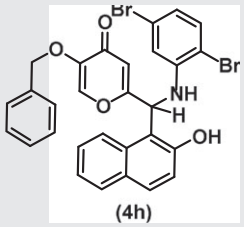 (4h) | 45 | 92 | 152–154 | 151–153[49] |
| 9 | 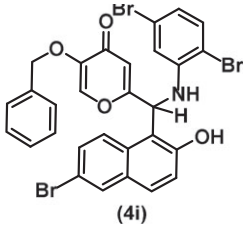 (4i) | 50 | 88 | 185–186 | 184–186[49] |
| 10 | 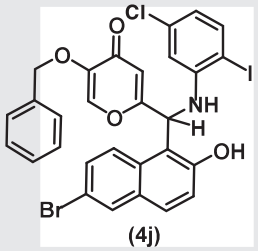 (4j) | 50 | 90 | 193–195 | 192–194[49] |

various temperatures and with various amounts of nanocatalyst to obtain a simple, rapid and efficient procedure for the synthesis of pyran-bearing Betti bases. As evident from Table 1, a variety of ionic liquids were used as catalysts in the model reaction under solvent-free conditions, and the results showed that $[Fe_3O_4@SiO_2@Triazol\text{-}Fc][HCO_3]$ is more efficient than other catalysts. Then a variety of conventional organic solvents such as $CHCl_3$, $CH_2Cl_2$, EtOH and water were screened for the model reaction in the presence of 10 mg of nanocatalyst at room temperature. Interestingly, the best result was achieved when EtOH–$H_2O$ (3:1) was used as solvent in the model reaction at room temperature (Table 1, entry 13). In continuation,

the model reaction was conducted using various quantities of nanocatalyst (10, 5 and 15 mg). It was observed that excellent yield was achieved using 10 mg of $[Fe_3O_4@SiO_2@Triazol\text{-}Fc][HCO_3]$ (Table 1, entry 13) and further decrease or increase in catalyst quantity did not increase the yield of the product significantly.

**TABLE 3** Synthesis of aryl(pyridinylamino)methyl-4*H*-pyran-4-one derivatives using 10 mg of $[Fe_3O_4@SiO_2@Triazol\text{-}Fc][HCO_3]$ nanocatalyst

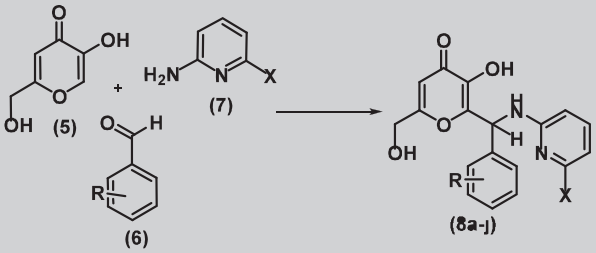


| Entry | Product | Time (min) | Yield (%) | Obs. m.p. (°C) | Lit. m.p. (°C) |
|---|---|---|---|---|---|
| 1 | 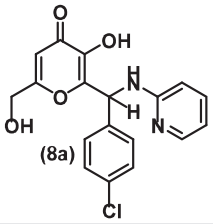 (8a) | 35 | 93 | 181–183 | 182–184[51] |
| 2 | 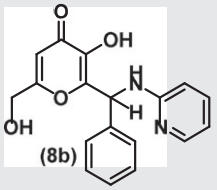 (8b) | 35 | 91 | 168–170 | 168–170[51] |
| 3 | 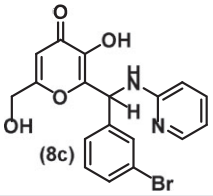 (8c) | 35 | 92 | 173–175 | 172–174[51] |
| 4 | 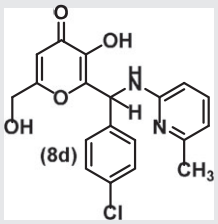 (8d) | 30 | 94 | 174–176 | 174–176[51] |
| 5 | 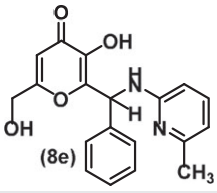 (8e) | 30 | 92 | 156–158 | 155–157[51] |
| 6 | 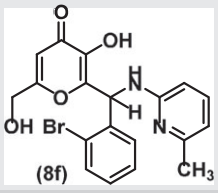 (8f) | 35 | 87 | 160–162 | 160–162[51] |

(Continues)

**TABLE 3** (Continued)

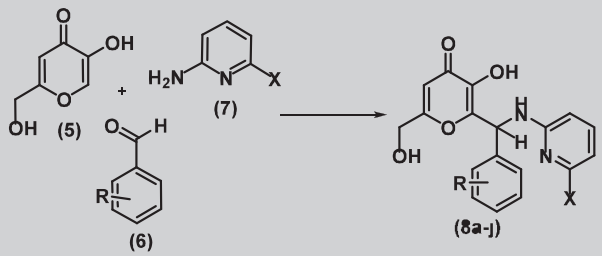


| Entry | Product | Time (min) | Yield (%) | Obs. m.p. (°C) | Lit. m.p. (°C) |
|---|---|---|---|---|---|
| 7 | 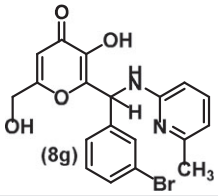 | 30 | 89 | 182–184 | 183–185[51] |
| 8 | 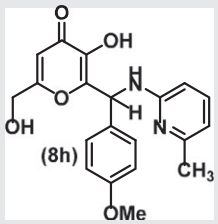 | 40 | 84 | 161–163 | 160–162[51] |
| 9 | 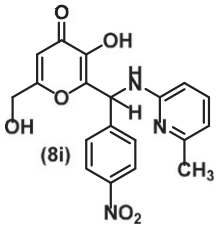 | 30 | 90 | 172–174 | 173–175[51] |
| 10 | 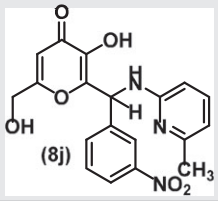 | 30 | 88 | 165–167 | 164–166[51] |

To demonstrate the scope and generality of the method, we designed and synthesized a new class of Betti bases bearing kojic acid scaffold. For this purpose, the three-component condensations of kojic aldehyde (**1**), 2-naphthols (**2**) and aniline derivatives (**3**) were investigated in the presence of the $[Fe_3O_4@SiO_2@Triazol\text{-}Fc][HCO_3]$ nanocatalyst (10 mg) at room temperature. As evident from Table 2, the reactions were carried out efficiently within 40–50 min and the corresponding products were afforded in good to high yields. All compounds were characterized using FT-IR, $^1H$ NMR and $^{13}C$ NMR spectroscopies and elemental analysis (C, H and N).

After establishing a general method for the synthesis of naphthopyran derivatives **4**, we tried to synthesize another important group of pyran-substituted Betti base derivatives **6** (Table 3). To achieve this aim, kojic acid was used instead of 2-naphthol in the traditional Betti reaction. Therefore, various aldehydes with either electron-donating or electron with-drawing groups were investigated under the optimized condition. According to the results summarized in Table 3, the three-component condensation completed within 30–40 min with high isolated yields.

The novel synthesized $[Fe_3O_4@SiO_2@Triazol\text{-}Fc][HCO_3]$ nanocatalyst has several basic and acidic active sites which could help the promotion of the reaction. $HCO_3$ is a Brønsted base site of the nanocatalyst which could activate nucleophiles. Consequently, acidic sites of the nanocatalyst increase the electrophilicity of the aldehydes and activate them to the nucleophilic attack. A plausible mechanism to explain these three-component reactions is presented in Scheme 3. The acid–base interactions among the nanocatalyst, aldehyde and amine lead

to the efficient reaction of aldehyde and amine derivatives, followed by dehydration and formation of related imine. In the next step, the catalyst activates 2-naphthol or kojic acid and, consequently, nucleophilic attack to the imine produces the desired products.

Furthermore, the reusability of the catalyst was investigated with the model reaction under modified conditions and the results are shown in Figure 5. After completion of the reaction, the catalyst was separated using an external magnet. The collected nanocatalyst was washed several times with EtOH prior to reuse. The recovered nanocatalyst could be reused for six runs without significant decrease in activity.

XRD and FT-IR analysis of the nanocatalyst after 6 runs of recycling were studied to prove the catalyst stability. According to the related data (Figure 6), significant changes in the nanocatalyst have not been observed after several uses.

To evaluate the stability of the [$Fe_3O_4$@$SiO_2$@Triazol-Fc][$HCO_3$] nanocatalyst under acidic conditions, 20 mg of nanoparticles was dispersed in 50 ml of HCl solution with a concentration of 0.1 M. After 24 h, the nanocatalyst was magnetically separated and the leached iron concentration was determined using atomic emission spectrometry. This experiment was also repeated for the recycled [$Fe_3O_4$@$SiO_2$@Triazol-Fc][$HCO_3$] nanocatalyst for comparison. The results showed that the leaching of iron from the nanoparticles was less than 1% which shows the

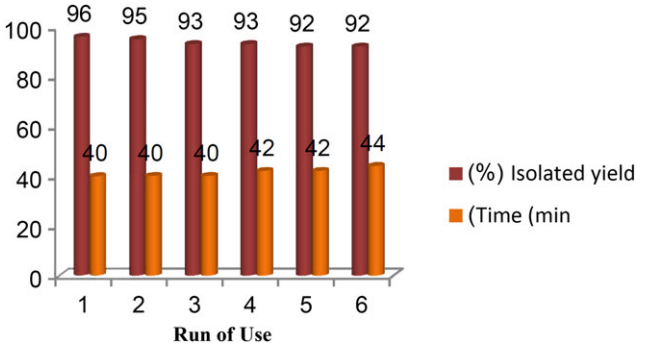


**FIGURE 5** Recyclability of [$Fe_3O_4$@$SiO_2$@Triazol-Fc][$HCO_3$] nanocatalyst in the synthesis of **4a**

stability of the nanocatalyst. The measured BET surface areas for $Fe_3O_4$, $Fe_3O_4$@$SiO_2$ and [$Fe_3O_4$@$SiO_2$@Triazol-Fc][$HCO_3$] nanoparticles are 76.4, 72.5 and 53.2 $m^2\ g^{-1}$, respectively. It is clear that $Fe_3O_4$ nanoparticles had the highest surface area. After coating with a layer of silica, the surface area slightly decreased and functionalization of the surface of $Fe_3O_4$@$SiO_2$ core–shell nanoparticles caused a further decrease in surface area to 53.2 $m^2\ g^{-1}$. The decrease of surface area may be because of an increase in the size of the particles and their agglomeration.

The magnetization curves measured for $Fe_3O_4$, [$Fe_3O_4$@$SiO_2$@Triazol-Fc][Cl] and [$Fe_3O_4$@$SiO_2$@Triazol-Fc][$HCO_3$] are compared in Figure 6. The saturation magnetization value was measured to be 68.0 emu $g^{-1}$

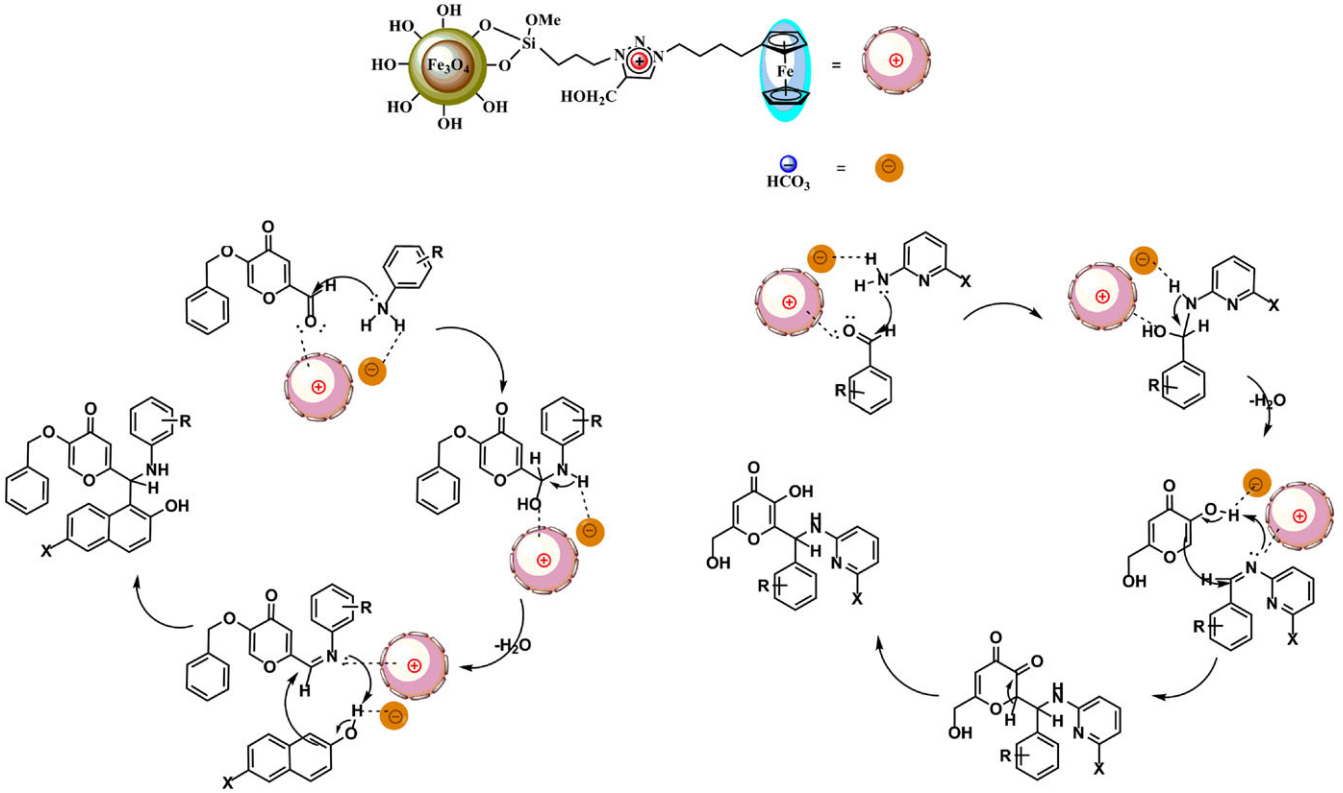


**SCHEME 3** Proposed mechanism for synthesis of products using [$Fe_3O_4$@$SiO_2$@Triazol-Fc][$HCO_3$] nanocatalyst

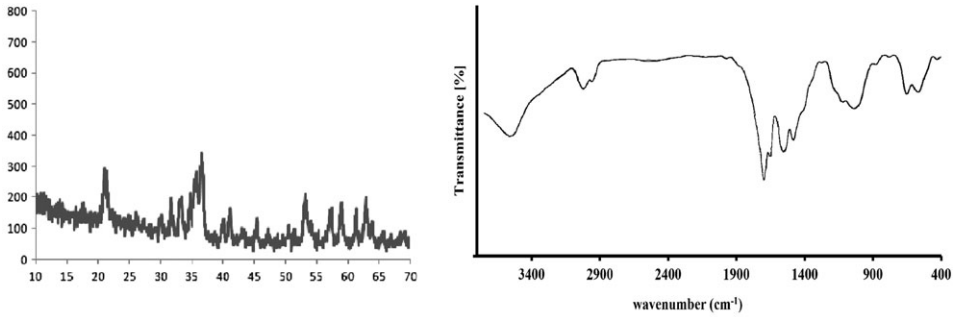


**FIGURE 6** XRD and FT-IR of the nanocatalyst after 6 times use

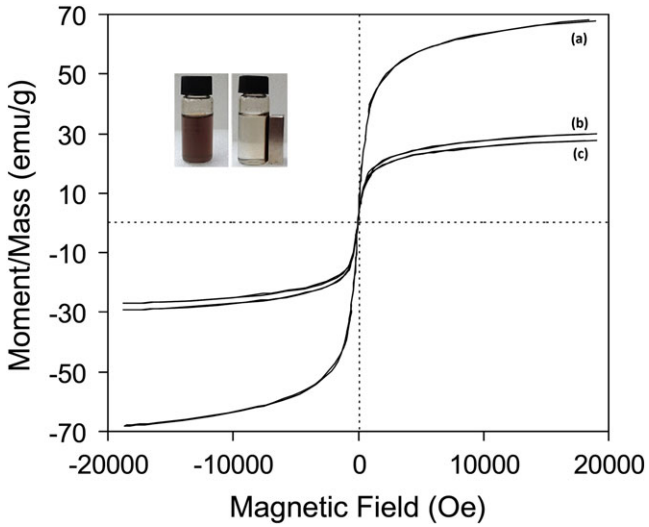


**FIGURE 7** Magnetization curves of (a) $Fe_3O_4$, (b) [$Fe_3O_4$@$SiO_2$@Triazol-Fc][Cl] and (c) [$Fe_3O_4$@$SiO_2$@Triazol-Fc][$HCO_3$] nanoparticles and photographs of magnetic separation of nanocatalyst with an external magnetic field

for $Fe_3O_4$. After being coated with silica and subsequent modifications, the saturated magnetization for [$Fe_3O_4$@$SiO_2$@Triazol-Fc][Cl] and [$Fe_3O_4$@$SiO_2$@Triazol-Fc][$HCO_3$] nanoparticles decreased to 28.5 and 26.2 emu $g^{-1}$, respectively. Although the saturation magnetization was reduced for the final nanocatalyst, complete magnetic separation of [$Fe_3O_4$@$SiO_2$@Triazol-Fc][$HCO_3$] nanoparticles was achieved using an external magnet.

## 3 | CONCLUSIONS

A new perspective on the synthesis of pyran-substituted Betti base derivatives has been introduced which could be applied in several fields of synthetic medicinal chemistry. In this context, novel [$Fe_3O_4$@$SiO_2$@Triazol-Fc][$HCO_3$] nanoparticles were synthesized, characterized and applied as an efficient heterogeneous catalyst for the synthesis of a wide variety of pyran-containing Betti base derivatives. A series of 2-hydroxynaphthalenyl(-arylamino)methyl-4*H*-pyran-4-one derivatives (**4a**–**j**) were synthesized via three-component condensation of kojic aldehyde, 2-naphthol and aniline derivatives catalysed by [$Fe_3O_4$@$SiO_2$@Triazol-Fc][$HCO_3$] nanoparticles at room temperature. Also aryl(pyridinylamino)methyl-4*H*-pyran-4-one derivatives (**8a**–**j**) were synthesized using the novel nanocatalyst via the one-pot three-component condensation reactions of various aromatic aldehydes, kojic acid and aminopyridine or methylaminopyridine in EtOH–$H_2O$ (3:1) at room temperature. In summary, a general, efficient and simple operation protocol using a novel recoverable magnetic nanocatalyst has been demonstrated to produce pyran-substituted Betti bases in short reaction times and good to high yields.

## 4 | EXPERIMENTAL

### 4.1 | Materials and apparatus

All of the chemical reagents used in this project were purchased from Merck and Sigma-Aldrich. A MEL-

TEMP model 1202D apparatus was used for the determination of melting points. A Bruker Tensor 27 spectrometer was applied for recording FT-IR spectra. The $^{1}$H NMR and $^{13}$C NMR spectra were recorded with a Bruker Spectrospin Avance 400 spectrometer. A Vario EL III analyser was applied for the of elementary analyses (C, H, N). XRD patterns of the nanoparticles were obtained with a Siemens D500 powder X-ray diffractometer (CuK radiation, $\lambda = 1.5406$ Å). EDX analysis and FE-SEM were conducted using a TESCAN MIRA3 field emission scanning electron microscope. TEM images were recorded with a Zeiss EM 10C electron microscope. BET surface areas of the nanoparticles were determined by $N_2$ adsorption/desorption with a BELSORP Mini II. Magnetization measurements were carried out with a model 155 alternative gradient force magnetometer at room temperature.

## 4.2 | Synthesis of [$Fe_3O_4$@$SiO_2$@Triazol-Fc][$HCO_3$] nanoparticles

### 4.2.1 | Synthesis of (1-(4-ferrocenylbutyl)-1*H*-1,2,3-triazol-4-yl)methanol

Propargyl alcohol (5 mmol), 4-chlorobutylferrocene (5 mmol) and sodium azide (5.2 mmol) were introduced in a 25 $cm^3$ round-bottomed flask in 8 ml od dimethylformamide. A catalytic amount of CuI (10 mol%) was then added and the reaction mixture was heated to 80°C for 12 h. The progress of the reaction was monitored by TLC until total conversion of the starting materials. After completion of the reaction, the product was extracted with EtOAc. The combined organic layers were dried over anhydrous $Na_2SO_4$, filtered and the solvent evaporated to afford the corresponding ferrocenyltriazole derivative. The residue was purified with silica column chromatography (*n*-hexane–ethyl acetate, 9:1, as eluent) to produce (1-(4-ferrocenylbutyl)-1*H*-1,2,3-triazol-4-yl)methanol. FT-IR ($cm^{-1}$): 3324, 3122, 2945, 2884, 1663, 1631, 1547. $^{1}$H NMR ($\delta$, ppm): 1.57–1.61 (m, 2H, &bond;$CH_2$&bond;), 1.66–1.73 (m, 2H, &bond;$CH_2$&bond;), 2.34 (t, $J = 7.5$ Hz, 2H, &bond;$CH_2$&bond;), 4.09–4.15 (m, 9H, CpH), 4.15–4.19 (m, 2H, &bond;$CH_2$&bond;), 4.62 (s, 2H, &bond;$CH_2$OH), 5.26 (bs, 1H, &bond;OH), 8.06 (s, 1H, triazole&bond;H). $^{13}$C NMR ($\delta$, ppm): 26.0, 27.0, 27.8, 55.7, 62.5, 66.0, 66.9, 67.4, 87.4, 128.7, 149.8.

### 4.2.2 | Synthesis of [$Fe_3O_4$@$SiO_2$@Triazol-Fc][Cl]

$Fe_3O_4$@$SiO_2$-propylchloride was prepared according to reported procedures.[46,47] Then, to a mixture of $Fe_3O_4$@$SiO_2(CH_2)_3Cl$ (1.0 g) in 10 ml of toluene, (1-(4-ferrocenylbutyl)-1*H*-1,2,3-triazol-4-yl)methanol (1.0 g) was added and the reaction mixture was heated at 80°C for 72 h. Then, the residue was filtered and washed with toluene (3 × 20 ml), MeOH (3 × 20 ml) and $CH_2Cl_2$ (3 × 20 ml) followed by drying under reduced pressure for 48 h at 40°C to afford the desired [$Fe_3O_4$@$SiO_2$@Triazol-Fc][Cl] nanoparticles.

### 4.2.3 | Synthesis of [$Fe_3O_4$@$SiO_2$@Triazol-Fc][$HCO_3$]

An amount of 0.2 g of sodium bicarbonate was dissolved in acetone–water (3:1, 40 ml) followed by the addition of [$Fe_3O_4$@$SiO_2$@Triazol-Fc][Cl] nanoparticles (0.2 g) and the reaction mixture was placed in an ultrasonic bath for 15 min. Then, the suspension was stirred using a mechanical stirrer for 24 h at room temperature. Target nanoparticles were separated from the reaction mixture using an external magnet and washed with water, EtOH and acetone. The desired nanocatalyst was then dried under vacuum and characterized using FT-IR spectroscopy, EDX analysis, XRD, FE-SEM and TEM.

## 4.3 | General procedure for synthesis of 2-hydroxynaphthalenyl(arylamino)methyl-4*H*-pyran-4-one derivatives (4a–j)

To a mixture of kojic aldehyde (1 mmol), 2-naphthol or 6-bromo-2-naphthol (1 mmol) and aniline derivative (1.1 mmol) in 4 ml of EtOH–$H_2O$ (3:1) was added [$Fe_3O_4$@$SiO_2$@Triazol-Fc][$HCO_3$] nanocatalyst (10 mg). The mixture was stirred at room temperature and the progress of the reaction was monitored by TLC (EtOAc–*n*-hexane, 1:4). After completion of the reaction, the catalyst was separated using an external magnet and the precipitate was collected by filtration and purified by recrystallization from EtOH. The separated nanocatalyst was washed with EtOH several times and dried for subsequent uses. The structures of newly synthesized compounds were characterized using FT-IR, $^{1}$H NMR and $^{13}$C NMR spectroscopies and CHN analysis.

## 4.4 | General procedure for synthesis of aryl(pyridinylamino)methyl-4*H*-pyran-4-one derivatives (8a–j)

To a mixture of kojic acid (1 mmol), aldehyde derivative (1 mmol) and aminopyridine or methylaminopyridine (1.1 mmol) in 4 ml of EtOH–$H_2O$ (3:1) was added [$Fe_3O_4$@$SiO_2$@Triazol-Fc][$HCO_3$] nanocatalyst (10 mg).

The mixture was stirred at room temperature and the progress of the reaction was monitored by TLC (EtOAc–n-hexane, 2:1). After completion of the reaction, the catalyst was separated using an external magnet and the precipitate was collected by filtration and purified by recrystallization from EtOH. The separated nanocatalyst was washed with EtOH several times and dried for subsequent uses.

## 4.5 | Characterization data

### 4.5.1 | 5-(Benzyloxy)-2-((2-hydroxynaphthalen-1-yl)(*p*-tolylamino)methyl)-4*H*-pyran-4-one (4a)

Pale yellow solid; m.p. 134–136°C. FT-IR (KBr, $cm^{-1}$): 3375, 3334, 3051, 2955, 1639, 1579, 1514, 1203. $^1$H NMR (400 MHz, $CDCl_3$, $\delta$, ppm): 2.26 (3H, s, $CH_3$), 4.98 (2H, 2 × d, $J$ = 12.4 Hz, benzylic-H), 5.12 (1H, s, NH), 6.21 (1H, s, methine-H), 6.67–6.70 (3H, m, Ar-H), 6.98 (2H, d, $J$ = 8.4 Hz, Ar-H), 7.23–7.25 (1H, m, Ar-H), 7.29–7.41 (6H, m, Ar-H), 7.51–7.55 (2H, m, Ar-H), 7.68 (1H, d, $J$ = 8.8 Hz, Ar-H), 7.81 (1H, d, $J$ = 8.0 Hz, Ar-H), 7.97 (1H, d, $J$ = 8.8 Hz, Ar-H), 10.61 (1H, bs, OH). $^{13}$C NMR (100 MHz, $CDCl_3$, $\delta$, ppm): 20.5, 55.7, 71.8, 112.7, 113.3, 115.1, 119.5, 121.3, 121.4, 123.1, 127.3, 127.7, 127.8, 128.5, 128.8, 128.9, 129.2, 129.6, 129.9, 130.1, 130.9, 132.1, 135.5, 141.4, 143.7, 147.0, 155.2, 167.7, 175.5. Anal. Calcd for $C_{30}H_{25}NO_4$ (%): C, 77.74; H, 5.44; N, 3.02. Found (%): C, 77.51; H, 5.46; N, 3.00.

### 4.5.2 | 5-(Benzyloxy)-2-[((4-chlorophenyl)amino)(2-hydroxynaphthalen-1-yl)methyl]-4*H*-pyran-4-one (4b)

Pale yellow solid; m.p. 145–147°C. FT-IR (KBr, $cm^{-1}$): 3361, 3342, 3049, 2928, 1633, 1608, 1516, 1218. $^1$H NMR (400 MHz, $CDCl_3$, $\delta$, ppm): 5.01 (2H, 2 × d, $J$ = 12.0 Hz, benzylic-H), 5.58 (1H, s, NH), 6.22 (1H, s, methine-H), 6.62 (2H, d, $J$ = 8.8 Hz, Ar-H), 6.77 (1H, s, Ar-H), 7.12 (2H, d, $J$ = 8.8 Hz, Ar-H), 7.26–7.29 (1H, m, Ar-H), 7.32–7.38 (6H, m, Ar-H), 7.52–7.58 (2H, m, Ar-H), 7.63 (1H, d, $J$ = 8.8 Hz, Ar-H), 7.80 (1H, d, $J$ = 8.0 Hz, Ar-H), 8.01 (1H, d, $J$ = 8.8 Hz, Ar-H), 10.43 (1H, bs, OH). $^{13}$C NMR (100 MHz, $CDCl_3$, $\delta$, ppm): 54.4, 71.8, 112.6, 113.2, 115.3, 119.2, 121.3, 123.2, 124.0, 127.4, 127.6, 128.6, 128.8, 128.9, 129.2, 129.3, 130.9, 132.1, 135.3, 141.6, 144.9, 146.9, 154.4, 168.5, 175.9. Anal. Calcd for $C_{29}H_{22}ClNO_4$ (%): C, 71.97; H, 4.58; N, 2.89. Found (%): C, 71.71; H, 4.59; N, 2.85.

### 4.5.3 | 5-(Benzyloxy)-2-[((3-chlorophenyl)amino)(2-hydroxynaphthalen-1-yl)methyl]-4*H*-pyran-4-one (4c)

Pale yellow solid; m.p. 138–140°C. FT-IR (KBr, $cm^{-1}$): 3351, 3298, 3045, 2984, 1632, 1546, 1219. $^1$H NMR (400 MHz, $CDCl_3$, $\delta$, ppm): 4.98 (2H, 2 × d, $J$ = 12.0 Hz, benzylic-H), 5.74 (1H, s, NH), 6.29 (1H, s, methine-H), 6.55–6.57 (1H, m, Ar-H), 6.70–6.78 (2H, s, Ar-H), 6.86 (1H, d, $J$ = 8.8 Hz, Ar-H), 7.08–7.13 (1H, m, Ar-H), 7.29–7.37 (7H, m, Ar-H), 7.50–7.57 (2H, m, Ar-H), 7.61–7.64 (1H, m, Ar-H), 7.79–7.81 (1H, m, Ar-H), 8.05–8.07 (1H, m, Ar-H), 10.43 (1H, bs, OH). $^{13}$C NMR (100 MHz, $CDCl_3$, $\delta$, ppm): 53.5, 71.9, 112.0, 112.3, 113.2, 113.7, 118.7, 119.1, 121.5, 123.2, 127.4, 127.6, 128.6, 128.8, 128.9, 129.2, 130.5, 130.9, 132.2, 135.2, 135.3, 141.7, 146.9, 147.7, 154.2, 169.2, 176.1. Anal. Calcd for $C_{29}H_{22}ClNO_4$ (%): C, 71.97; H, 4.58; N, 2.89. Found (%): C, 71.73; H, 4.60; N, 2.86.

### 4.5.4 | 5-(Benzyloxy)-2-[((5-chloro-2-iodophenyl)amino)(2-hydroxynaphthalen-1-yl)methyl]-4*H*-pyran-4-one (4d)

Pale yellow solid; m.p. 158–160°C. FT-IR (KBr, $cm^{-1}$): 3345, 3278, 3063, 2874, 1637, 1577, 1505, 1208. $^1$H NMR (400 MHz, $CDCl_3$, $\delta$, ppm): 4.99 (2H, 2d, $J$ = 12.2 Hz, benzylic-H), 6.27 (1H, d, $J$ = 6.9 Hz, methine-H), 6.47–6.49 (1H, m, Ar-H), 6.57 (1H, s, pyrone-H), 6.67 (1H, s, N-H), 7.03 (1H, s, Ar-H), 7.28–7.36 (7H, m, Ar-H), 7.46 (1H, d, $J$ = 8.2 Hz, Ar-H), 7.52–7.60 (3H, m, Ar-H, pyrone-H), 7.74 (1H, d, $J$ = 8.1 Hz, Ar-H), 8.10 (1H, d, $J$ = 8.7 Hz, Ar-H), 10.81 (1H, s, OH). $^{13}$C NMR (100 MHz, $CDCl_3$, $\delta$, ppm): 52.1, 82.5, 70.9, 109.4, 110.7, 112.6, 117.9, 118.3, 120.6, 122.0, 126.3, 126.6, 127.5, 127.7, 127.9, 128.2, 129.9, 131.1, 134.3, 134.4, 138.9, 140.8, 145.9, 145.9, 152.9, 168.1, 175.4. Anal. Calcd for $C_{29}H_{21}ClINO_4$ (%): C, 57.12; H, 3.47; N, 2.30. Found (%): C, 56.88; H, 3.48; N, 2.31.

### 4.5.5 | 5-(Benzyloxy)-2-((6-bromo-2-hydroxynaphthalen-1-yl)((2-bromophenyl)amino)methyl)-4*H*-pyran-4-one (4e)

Pale yellow solid; m.p. 152–154°C. FT-IR (KBr, $cm^{-1}$): 3389, 3342, 3066, 2925, 1637, 1576, 1499, 1206. $^1$H NMR (400 MHz, $CDCl_3$, $\delta$, ppm):4.92 (2H, 2d, $J$ = 12.4 Hz, benzylic-H), 6.22 (2H, s, methine-H, N&bond;H), 6.55–6.59 (2H, m, Ar-H), 6.78 (1H, s, pyrone-H), 7.05 (1H, t, $J$ = 7.8 Hz, Ar-H), 7.20–7.31 (7H, m, Ar-H), 7.36 (1H, d, $J$ = 8.8 Hz, Ar-H), 7.47 (1H, dd, $J$ = 9.1 Hz, $J$ = 1.5 Hz, Ar-H), 7.51 (1H, s, pyrone-H), 7.79 (1H, d, $J$ = 1.5 Hz,

Ar-H), 7.88 (1H, d, $J$ = 9.1 Hz, Ar-H), 10.63 (1H, s, OH). $^{13}$C NMR (100 MHz, $CDCl_3$, $\delta$, ppm): 52.3, 70.9, 110.0, 110.9, 111.1, 113.1, 115.5, 118.3, 119.1, 122.4, 126.6, 127.5, 127.7, 128.8, 129.1, 129.3, 129.7, 130.0, 131.8, 134.3, 140.8, 142.3, 145.9, 153.4, 167.7, 175.1. Anal. Calcd for $C_{29}H_{21}Br_2NO_4$ (%): C, 57.36; H, 3.49; N, 2.31. Found (%): C, 57.11; H, 3.51; N, 2.30.

## ACKNOWLEDGEMENTS

The authors acknowledge financial support from the Iran National Science Foundation (INSF) and the University of Tabriz.

## ORCID

*Kazem D. Safa* https://orcid.org/0000-0003-4550-9751
*Reza Teimuri-Mofrad* https://orcid.org/0000-0002-5812-6445

## REFERENCES

[1] J. E. Mondloch, E. Bayram, R. G. Finke, *J. Mol. Catal. A* **2012**, *355*, 1.

[2] P. Munnik, P. E. de Jongh, K. P. de Jong, *Chem. Rev.* **2015**, *115*, 6687.

[3] J. A. Widegren, R. G. Finke, *J. Mol. Catal. A* **2003**, *198*, 317.

[4] J. M. Thomas, R. Raja, *Annu. Rev. Mater. Res.* **2005**, *35*, 315.

[5] M. B. Gawande, P. S. Branco, R. S. Varma, *Chem. Soc. Rev.* **2013**, *42*, 3371.

[6] V. Polshettiwar, R. S. Varma, *Green Chem.* **2010**, *12*, 743.

[7] M. Haruta, *Catal. Today* **1997**, *36*, 153.

[8] S. Shylesh, V. Schünemann, W. R. Thiel, *Angew. Chem. Int. Ed.* **2010**, *49*, 3428.

[9] V. Polshettiwar, R. Luque, A. Fihri, H. Zhu, M. Bouhrara, J. M. Basset, *Chem. Rev.* **2011**, *111*, 3036.

[10] D. Wang, D. Astruc, *Chem. Rev.* **2014**, *114*, 6949.

[11] B. Karimi, F. Mansouri, H. M. Mirzaei, *ChemCatChem* **2015**, *7*, 1736.

[12] R. N. Baig, R. S. Varma, *Chem. Commun.* **2013**, *49*, 752.

[13] M. A. Zolfigol, R. Ayazi-Nasrabadi, S. Baghery, *Appl. Organometal. Chem.* **2016**, *30*, 500.

[14] M. A. Zolfigol, R. Ayazi-Nasrabadi, S. Baghery, *Appl. Organometal. Chem.* **2016**, *30*, 273.

[15] R. Dalpozzo, *Green Chem.* **2015**, *17*, 3671.

[16] A. Maleki, M. Aghaei, N. Ghamari, *Appl. Organometal. Chem.* **2016**, *30*, 939.

[17] A. Maleki, E. Akhlaghi, R. Paydar, *Appl. Organometal. Chem.* **2016**, *30*, 382.

[18] A. Shahrisa, S. Esmati, *Synlett* **2013**, *24*, 595.

[19] J. Zhu, H. Bienayme, *Multicomponent Reactions*, Wiley-VCH, Weinheim **2005** 121.

[20] A. Shahrisa, R. Teimuri-Mofrad, M. Gholamhosseini-Nazari, *Synlett* **2015**, *26*, 1031.

[21] C. Cardellicchio, M. A. M. Capozzi, F. Naso, *Tetrahedron: Asymmetry* **2010**, *21*, 507.

[22] I. Szatmári, F. Fülöp, *Tetrahedron* **2013**, *69*, 1255.

[23] A. Kumar, M. K. Gupta, M. Kumar, *Tetrahedron Lett.* **2010**, *51*, 1582.

[24] B. Karmakar, J. A. Banerji, *Tetrahedron Lett.* **2011**, *52*, 4957.

[25] S. D. Dindulkar, V. G. Puranik, Y. T. Jeong, *Tetrahedron Lett.* **2012**, *53*, 4376.

[26] K. M. Khandarkar, M. D. Shanti, M. Ahmed, J. S. Meshram, *J. Chem. Sci.* **2013**, *125*, 1573.

[27] N. Gyémánt, H. Eng, Z. Schelz, I. Szatmári, D. Tóth, F. Fülöp, J. Molnár, P. De Witte, *Br. J. Cancer* **2010**, *103*, 178.

[28] A. Y. Shen, C. T. Tsai, C. L. Chen, *Eur. J. Med. Chem.* **1999**, *34*, 877.

[29] I. Szatmári, A. Hetényi, L. Lázár, F. Fülöp, *J. Heterocycl. Chem.* **2004**, *41*, 367.

[30] M. L. Deb, B. S. Saikia, K. Borah, P. K. Baruah, *Synth. Commun.* **2016**, *46*, 1940.

[31] M. Heydenreich, A. Koch, S. Klod, I. Szatmári, F. Fülöp, E. Kleinpeter, *Tetrahedron* **2006**, *62*, 11081.

[32] I. Szatmári, T. A. Martinek, L. Lázár, A. Koch, E. Kleinpeter, K. Neuvonen, F. Fülöp, *J. Org. Chem.* **2004**, *69*, 3645.

[33] M. Marinova, K. Kostova, P. Tzvetkova, M. Tavlinova-Kirilova, A. Chimov, R. Nikolova, B. Shivachev, V. Dimitrov, *Tetrahedron: Asymmetry* **2013**, *24*, 1453.

[34] M. He, N. Yang, C. Sun, X. Yao, M. Yang, *Med. Chem. Res.* **2011**, *20*, 200.

[35] R. Schiller, L. Tichotová, J. Pavlík, V. Buchta, B. Melichar, I. Votruba, J. Kuneš, M. Špulák, M. Pour, *Bioorg. Med. Chem. Lett.* **2010**, *20*, 7358.

[36] H. Hussain, S. Aziz, B. Schulz, K. Krohn, *Nat. Prod. Commun.* **2011**, *6*, 841.

[37] S. Wang, G. Milne, X. Yan, I. J. Posey, M. C. Nicklaus, L. Graham, W. G. Rice, *J. Med. Chem.* **1996**, *39*, 2047.

[38] S. S. Bisht, N. Jaiswal, A. Sharma, S. Fatima, R. Sharma, N. Rahuja, A. Srivastava, V. Bajpai, B. Kumar, R. P. Tripathi, *Carbohydr. Res.* **2011**, *346*, 1191.

[39] Y. Wang, S. -Y. Mo, S. -J. Wang, S. Li, Y. -C. Yang, J. -G. Shi, *Org. Lett.* **2005**, *7*, 1675.

[40] D. Kumar, P. Sharma, H. Singh, K. Nepali, G. K. Gupta, S. K. Jain, F. Ntie-Kang, *RSC Adv.* **2017**, *7*, 36977.

[41] M. Zirak, B. Eftekhari-Sis, *Turk. J. Chem.* **2015**, *39*, 439.

[42] A. P. D. Rodrigues, A. S. C. Carvalho, A. S. Santos, C. N. Alves, J. L. M. Nascimento, E. O. Silva, *Cell Biol. Int.* **2011**, *35*, 335.

[43] A. Shahrisa, K. D. Safa, S. Esmati, *Spectrochim. Acta A* **2014**, *117*, 614.

[44] K. D. Safa, H. Mousazadeh, *Monatsh. Chem.* **2016**, *147*, 1951.

[45] R. Teimuri-Mofrad, M. Gholamhosseini-Nazari, E. Payami, S. Esmati, *Res. Chem. Intermed.* **2017**, *43*, 7105.

[46] R. Teimuri-Mofrad, M. Gholamhosseini-Nazari, E. Payami, S. Esmati, *Appl. Organometal. Chem.* **2018**, *32*, e3955.

[47] R. Teimuri-Mofrad, S. Esmati, M. Rabiei, M. Gholamhosseini-Nazari, *Heterocycl. Commun.* **2017**, *23*, 439.

[48] R. Teimuri-Mofrad, S. Esmati, M. Rabiei, M. Gholamhosseini-Nazari, *J. Chem. Res.* **2018**, *42*, 7.

[49] R. Teimuri-Mofrad, M. Gholamhosseini-Nazari, S. Esmati, A. Shahrisa, *J. Chem. Sci.* **2017**, *129*, 1449.

[50] A. Shahrisa, R. Teimuri-Mofrad, M. Gholamhosseini-Nazari, *Mol. Diversity* **2015**, *19*, 87.

[51] R. Teimuri-Mofrad, A. Shahrisa, M. Gholamhosseini-Nazari, N. Arsalani, *Res. Chem. Intermed.* **2016**, *42*, 3425.

[52] R. Teimuri-Mofrad, I. Ahadzadeh, M. Gholamhosseini-Nazari, S. Esmati, A. Shahrisa, *Res. Chem. Intermed.* **2018**, *44*, 2913.

[53] R. Teimuri-Mofrad, M. Gholamhosseini-Nazari, S. Esmati, A. Shahrisa, *Res. Chem. Intermed.* **2017**, *43*, 6845.

**How to cite this article:** Gholamhosseini-Nazari M, Esmati S, Safa KD, Khataee A, Teimuri-Mofrad R. Synthesis and application of novel 1,2,3-triazolylferrocene-containing ionic liquid supported on $Fe_3O_4$ nanocatalyst in the synthesis of new pyran-substituted Betti bases. *Appl Organometal Chem*. 2019;e4701. https://doi.org/10.1002/aoc.4701